Egypt. J. Chem. **Vol. 64**, No. 1 pp. 487 - 494 (2021)

Egyptian Journal of Chemistry

http://ejchem.journals.ekb.eg/

Microstructure and Dielectric Properties of Polyaniline Doped with Copper Nanoparticles

Juman A. Naser*, Zainab W. Ahmed, Wedad J. Fendi

Department of Chemistry, College of Education for Pure Science- Ibn Al-Haitham, University of Baghdad, Baghdad, Iraq

Abstract

Polyaniline (PANI) has been prepared by the oxidation method in order to fabricate it with various concentrations of copper nanoparticles (CuNPs) which produced using the reduction method. Various techniques have characterized pure PANI and PANI doped CuNPs composites, such as fourier transform infrared spectroscopy (FT-IR), X-ray diffraction spectroscopy (XRD), field emission scanning electron microscopy (FE-SEM) and energy dispersive X-ray spectroscopy (EDS), which were provided important information about the structure and morphology of the fabricated polymer nanocomposites. The properties of dielectric permittivity (Ɛ′), dielectric loss (Ɛ″) and electrical conductivity (σ_{AC}) properties were studied at room temperature versus a range of frequency (15-150) kHz. The results demonstrated that the addition of copper nanoparticles to polyaniline matrix increases the dielectric permittivity property and it decreases with increasing the frequency to reach a fixed value. So, the electrical conductivity of studied samples decrease with increasing the frequency.

Keywords: Polyaniline; Copper nanoparticles; Nanocomposites; Dielectric permittivity; Dielectric loss; Electrical conductivity.

1. Introduction

Conductive polymers are important materials, since in addition to the mechanical properties that are found in conventional polymers they have magnetic, electrical and optical properties [1]. Polyaniline (PANI) is considered one of the most promising and distinctive polymers, as it has received attention nowadays because it is easy to prepare, low cost, high stability and conductivity, which made it have wide applications in the field of batteries, sensors, transistors, electrical circuits and electrical or optical devices [2-7].

To produce composite materials with improved physical parameters, the combination of the special properties of conductive polymers with different nanoparticles is predictable. Despite the proven application of conductive polymer nanocomposites in various technological aspects, there are few reports of their structure, morphology and electrical or optical characteristics [8, 9]. Important studies have been conducted on polyaniline doped with nanoparticles by many researchers [10-13]. Therefore, no study on the dielectrical properties of PANI doped CuNPs composites has been reported. Hence, to determine new properties arising from the molecular interactions of these two different chemical compounds of PANI and CuNPs were prepared in this work.

Copper nanoparticles (CuNPs) can be prepared by various physical and chemical methods such as laser ablation, microwave irradiation, chemical reduction, electroreduction process and polyol method [14-18]. The chemical reduction is one of the most prominent economic, simple and rapid methods for preparing nanoparticles. It is also a preferred method for the distribution of nanoparticles by controlling physical experiment factors [19]. CuNPs have been applied in the field of catalysts, solar cells, sensors and antibacterials [20-24]. Their electrical, thermal and optical properties make copper nanoparticles an attractive material.

*Corresponding author e-mail: juman_chem@yahoo.com.; juman.a.n@ihcoedu.uobaghdad.edu.iq.
Receive Date: 08 August 2020, Revise Date: 25 November 2020, Accept Date: 06 December 2020
DOI: 10.21608/EJCHEM.2020.38507.2793

In recent years, metallic nanoparticles are extensively investigated for different fields of technology and many applications including noble nanoparticles such as gold and silver, but they are costly [25-27]. Thus, copper nanoparticles are excellent alternative substance.

In this work, PANI and various concentrations of PANI doped CuNPs composites were prepared and investigated the dependence of dielectric permittivity, dielectric loss and electrical conductivity properties with the frequency at room temperature. The pure PANI, CuNPs and PANI doped CuNPs samples were characterized using FT-IR, XRD, FE-SEM and EDS.

2.Experimental

2.1. Materials

Aniline, ammonium persulfate, copper sulfate pentahydrate, citric acid, sodium borohydride and ethanol were supplied from Sigma Aldrich Company. The aqueous solutions were prepared using distilled water.

2.2. Methods

2.2.1. Preparation of Polyaniline (PANI)

PANI was prepared by the chemical oxidative polymerization [28]. A double distilled aniline C_6H_7N (10 mL) was dissolved in a (125 mL) (1 N) of HCl solution with stirring for ½ h at room temperature. After that a (60 mL) (1M) of an aqueous solution of ammonium persulfate $(NH_4)_2S_2O_8$ was added as an oxidant through the dropwise with the continuous stirring for 4 h. The reaction mixture was left at a range (0–5) °C with the continuous stirring for 7 h, and then kept at room temperature overnight. The precipitated polymer has been filtered and washed several times with distilled water and methanol to remove the oligomer. Hence, the precipitated product was dried at 60 °C for 6 h and grind to be a powder.

2.2.2. Preparation of copper nanoparticles (CuNPs)

Copper nanoparticles was prepared by the chemical reduction method [29]. A (900 mL) (0.006 M) of copper sulfate pentahydrate $CuSO_4.5H_2O$ was mixed with a (900 mL) (0.006 M) of an aqueous solution of citric acid $C_6H_8O_7$ as a stabilizer at room temperature. The mixture was heated to 80 °C with the continuous stirring. Then, a (450 mL) (0.012 M) of sodium borohydride $NaBH_4$ was added to the previous mixture as a reducing agent drop by drop while maintaining the same experimental conditions. After addition, the mixture was left with the continuous stirring for 2 h and set at 80 °C. The obtained product was washed several times with the distilled water to remove the residual reactants and dried in a vacuum oven at 70 °C. Finally, it was transferred to a furnace at 350 °C for 2 h.

2.2.3. Preparation of PANI doped CuNPs

PANI was doped with a weight percentages 1, 2, 3, 4 and 5 %wt of CuNPs. The obtained percentages were sonicated with ethanol for ½ h and dried for 1 h in a vacuum oven at 70 ºC.

2.2.4. Preparation of the samples

The pure PANI and PANI doped CuNPs samples were compressed as pellets by applying a pressure of 2 ton on them using a hydraulic piston for a period of ½ h. The pellet had a diameter 1 cm and a thickness were and 0.3 cm, Fig. 1.

Fig. 1. Image of the compressed sample.

2.3. Characterization

The characterization of the pure PANI and PANI doped CuNPs samples were done. Fourier transform infrared (FT-IR) spectrums were measured by KBr pellets within the range (400–4000) cm^{-1} using Shimadzu 8000S FT-IR spectrometer. The X-ray diffraction analysis was recorded by Shimadzu X-ray diffractometer XRD-6000. Field emission scanning electron microscopy (FE-SEM) and energy dispersive X-ray spectroscopy (EDX) were performed using Tescan VEGA3 microscope. Dielectric measurements were used by inductance (L), capacitance (C), and resistance (R) (LCR) meter Instek LCR-8101G.

3. Results and Discussion

3.1. FT-IR spectroscopy

The chemical compositions of the pure PANI, CuNPs and PANI doped CuNPs sample (5%) were performed by FT-IR spectroscopy, as shown in Fig. 2. The peaks at 833, 1186, 1221, 1400, 1558 and 3118 cm^{-1} due to the characteristic absorption of

PANI were shown in the recorded FT-IR spectrum of pure PANI, Fig. 2(a). So, the peaks at 1558 cm^{-1} and 1489 cm^{-1} are due to the symmetric and asymmetric stretching vibrations of C-C bond in the ring. The peaks at 1400 cm^{-1} and 1304 cm^{-1} are attributed to the bending vibration of N-H and C-C bond respectively. As the peaks at 1221 cm^{-1} and 1186 cm^{-1} are attributed to the bending vibrations of C-H bond in plane and out of plane respectively, Fig. 2(a).

The spectrum of the prepared CuNPs are shown in Fig. 2(b). A broad band is observed at the region 3475 cm^{-1} and 1641 cm^{-1} are due to the stretching and bending vibration respectively of hydroxyl group O-H of the adsorbed water on the nanoparticles surfaces. The presence of a band at low frequency 619 cm^{-1} is almost due to vibration of the Cu-O group, which confirms the physical bonding of water molecules with the surface of CuNPs.

Fig. 2(c) shows the FT-IR spectrum of PANI doped with CuNPs sample (5%). It is observed that it has the same absorption peaks of pure PANI but that shifted to higher frequencies. This shifting in the peaks confirms the occurred interactions between CuNPs and PANI. So, it is noticeable that the absorption peaks are appeared at 621 cm^{-1}, 498 cm^{-1} and 445 cm^{-1} attributed to Cu-OH, Cu-O-Cu and free O-H group, respectively. Also noticed that there is a distinctive peak at 621 cm^{-1}, it can be returned to Cu-N bond.

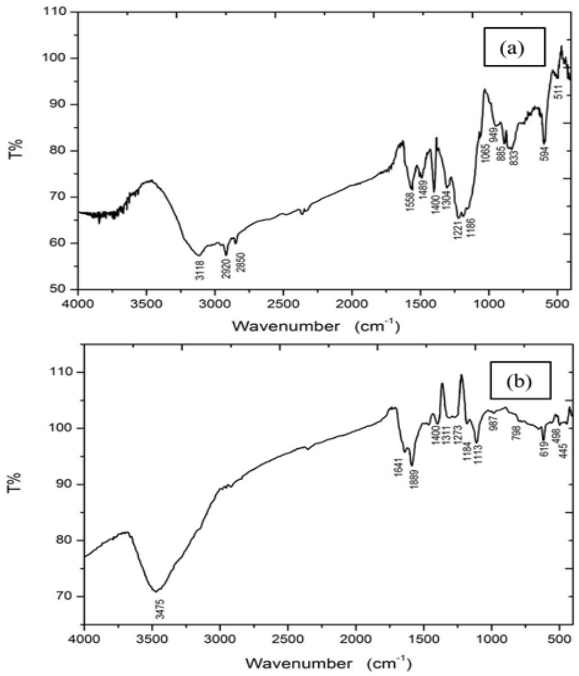

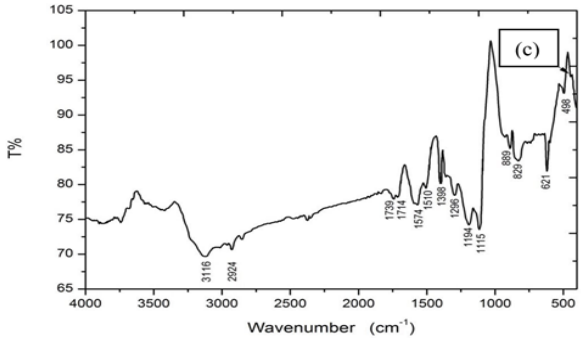

Fig. 2. FT-IR spectrum of; (a): PANI, (b): CuNPs and (c): PANI doped with CuNPs sample (5%).

3.2. XRD spectroscopy

The crystalline structure and phase components of pure PANI, CuNPs and PANI doped CuNPs sample (5%) was characterized by X-ray diffraction analysis as shown in Fig. 4. The XRD diffraction patterns of pure PANI is shown in Fig. 3(a). The characteristic peaks which appeared at angles 15.3, 22.4 and 26.28 correspond to the crystal planes of PANI (011), (020) and (200). These arose peaks are attributed to the regular aniline repetition.

The prepared CuNPs were examined by XRD technique also, as shown in Fig. 3(b). The diffraction reflections showed at the angles 22.9469° 43.4329° and 74.2120° with high intensities that matched the lattice planes (111), (200) and (220) respectively. This indicates the face-centered cubic structure of CuNPs which in agreement with the literatures [30]. So, the recorded diffraction patterns correspond the standard data in (JCPDS) card No.85-1326.

The average value of prepared nanoparticles size were determined utilizing Debye-Scherrer equation [31]:

$$L = 0.94\,\lambda / \beta \cos \Theta \quad \text{..... (1)}$$

where L is the particle size, λ = 0.167Aº is the wavelength of X-ray, β is the full width value at half maximum of the intensity (in radian) and ɵ is the Bragg angle (in degree). It was found that the calculated crystalline size of prepared nanoparticles was about 29.5 nm.

Fig. 5(c) shows XRD patterns of the PANI doped with CuNPs sample (5%). It is showed a crystalline structure where the peaks seems more sharp intensity compared to PANI, as a result to the high dispersion of nanoparticles in PANI.

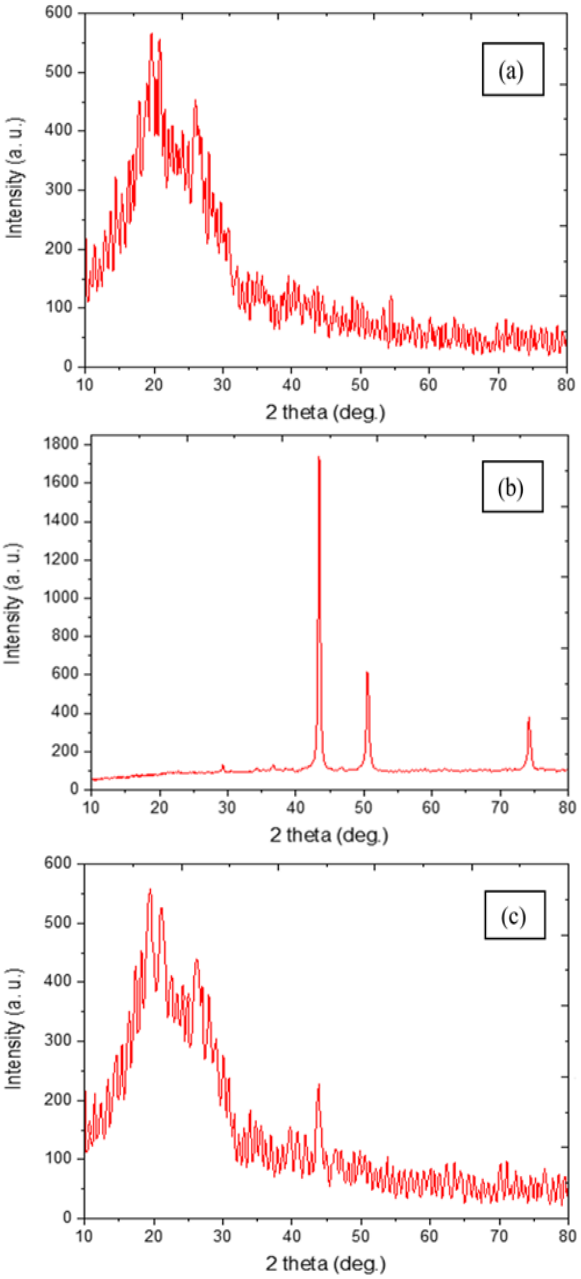

Fig. 3. XRD patterns of; (a): PANI, (b): CuNPs and (c): PANI doped with CuNPs sample (5%).

3.3. FE-SEM microscopy

The field emission scanning electron microscopy was used to study the morphology of pure PANI, CuNPs and PANI doped CuNPs sample (5%), as shown in Fig. 4. The micrograph of pure PANI shows uniformly a homogeneous structure with sponge-like shape, Fig. 4(a). The FE-SEM observation reflects ownership of the prepared CuNPs to a cubic shape and their aggregation in high densities with a range of the particle sizes ≃30 nm (±10) which also agrees with the X-ray diffraction result of CuNPs sample, Fig. 4(b). The surface morphology of PANI doped CuNPs sample was shown in Fig. 4(c), it can be seen the distribution uniformity of nanoparticles in the matrix of PANI [28], which confirms the good dispersion. Hence, the dopant nanoparticles are coated with the polymer matrix and the microscopic structure takes a granular shape, which agrees with the result of the X-ray diffraction.

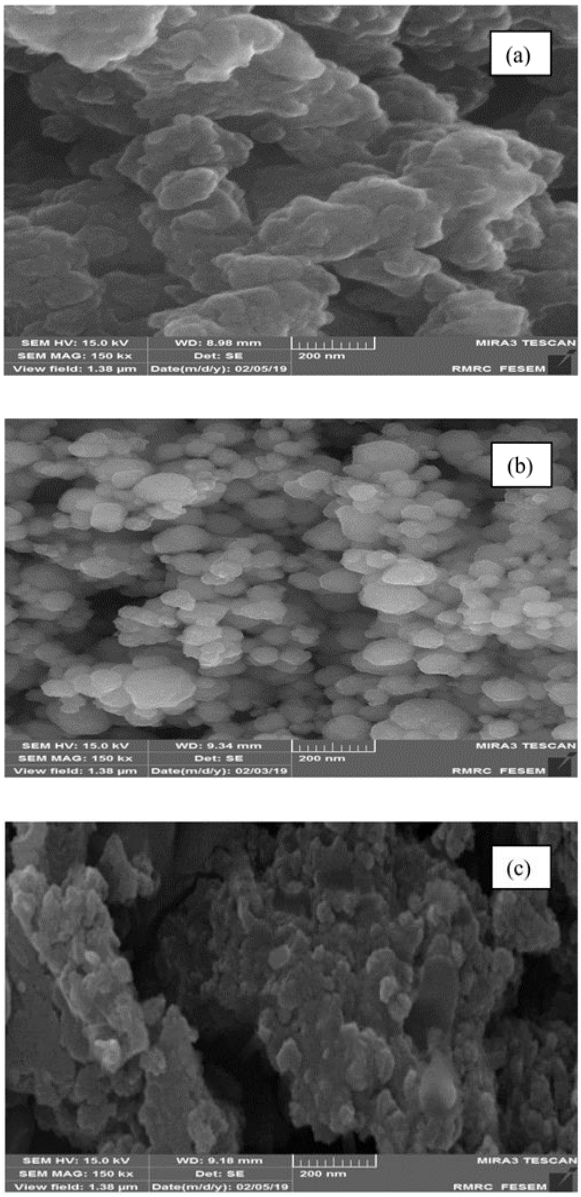

Fig. 4. FE-SEM micrograph of; (a): PANI, (b): CuNPs and (c): PANI doped with CuNPs sample (5%).

3.4. EDS spectroscopy

The X-ray dispersion spectroscopy (EDS) of pure PANI, CuNPs and PANI doped CuNPs sample (5%) was investigated, as shown in Fig. 5. The result in Fig. 5(a) confirms that the structure of the prepared

PANI contained carbon and nitrogen, which indicates the reliability and purity of the produced polymer. It is noticed that the prepared CuNPs was pure without any impurities, Fig. 5(b). Thus, no peak returned to any impurities in the spectrum, only copper and oxygen trace has been detected which are returned to the oxide layer on the surface of nanoparticles as a result of exposure to the atmosphere. This further assured that the prepared CuNPs. In addition, the analysis of PANI doped CuNPs sample confirms the incorporation of nanoparticles into the polymer matrix and a peak intensity of copper element was observed, Fig. 5(c).

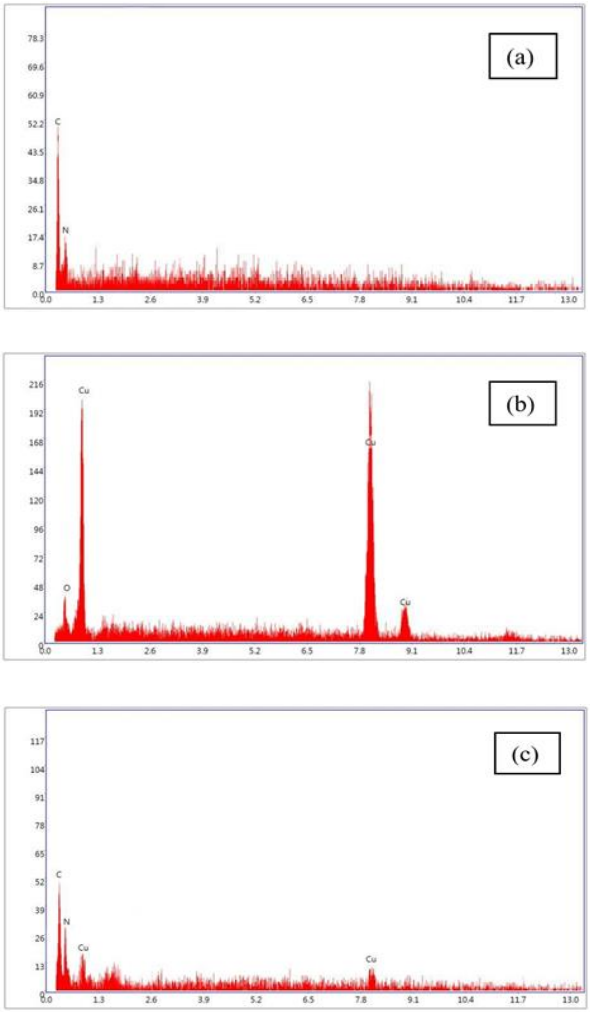

Fig. 5. EDS spectrum of; (a): PANI, (b): CuNPs and (c): PANI doped with CuNPs sample (5%).

3.5. Dielectric measurements

The dielectric permittivity property of polymer nanocomposites depend on the type of polymer, nanomaterials and dopant in addition to the frequency. The dielectric parameters of pure PANI, CuNPs and PANI doped CuNPs samples were described by measuring the dielectric permittivity properties versus a range of frequency (15-150) kHz. The values of the real dielectric permittivity (Ɛ′) were estimated by the measured capacitance (C) according to the relationship (2) [32]:

$$Ɛ' = C\,d\,/\,Ɛ^{o}\,A \quad \text{..... (2)}$$

where A is the electrode area (m^2), d is the sample thickness (m) and $Ɛ^{o}$ is the free space permittivity (8.85×10^{-12}/N m^2).

The values of imaginary dielectric permittivity (Ɛ″) were described as the following equation (3) [33]:

$$Ɛ'' = tan\,\delta\,.\,Ɛ' \quad \text{..... (3)}$$

where $tan\,\delta$ is the lost angle which was founded using the equation (4) [34]:

$$tan\,\delta = 1\,/\,w\,R\,C \quad \text{..... (4)}$$

where w is the angular frequency ($w = 2\,\pi\,f$), f is the applied frequency of electric field and R is the resistance of sample (Ohm).

The electrical conductivity σ_{AC} values have been estimated using the following expression (5) [35]:

$$\sigma_{AC} = Ɛ^{o}\,Ɛ''\,w \quad \text{..... (5)}$$

The behavior of real Ɛ′ and imaginary Ɛ″ dielectric permittivity as a function of the frequency for pure PANI and PANI doped CuNPs samples at a range of frequencies (15-150) kHz at room temperature are shown in Fig. 6. The value of real dielectric permittivity was found to be high at low frequencies and slowly decreased with increasing the frequency until it was almost constant at high frequencies, as a result to the interfacial polarization in the tested samples, Fig. 6(a). It can be due to the presence of electrical heterogeneous materials such as PANI and CuNPs [35]. It is also noted that the real dielectric permittivity of PANI increases with the increase in the dopant ratio, which is due to the possession of CuNPs of a distinct polarity that enhances the value of total polarization which consequently leads to an increase in the value of real dielectric permittivity that attributed to the increasing of system polarization [36]. The applied electric field creates a high induced polarization in the species, which products a high dielectric permittivity. So, at high frequencies range the polarized species cannot follow the applied field, then the dielectric permittivity becomes low values [37].

Continuously, the values of imaginary dielectric permittivity or dielectric loss Ɛ″ versus the frequency range for pure PANI and PANI doped CuNPs samples are shown in Fig. 6(b). It was observed that

with increasing the studied frequency, all the values of the imaginary dielectric permittivity also decreased, and found to be constant at high frequencies. A decrease in the frequency alternation leads to the polarization orientation in the polar groups of doped polymer systems. On the other hand, it can be observed that the values of dielectric loss ε̈ decrease with increasing a ratio of CuNPs in the polymer matrix, which led to increasing their contribution in raising of the conductivity values, because of the concentration increasing of charge carriers [38].

The dependence of electrical conductivity σ_{AC} on the frequency for pure PANI and PANI doped CuNPs samples at the same range of frequencies (15-150) kHz also are investigated, Fig. 6(c). The electrical conductivity curves show a slow increasing in conductivity at the frequency range (10-50) kHz as these values seem constant in the range (50-15) kHz. The slow increasing can be attributed to the charge carriers which are transported during the jumping operations where a subsidence in jumping occurs when the frequencies increase during the polymer chains. Thus, the conductivity of the polymer doped samples increases with the ratio increasing of CuNPs. This behavior can be due to the increase in the number of charge carriers (protons and electrons) provided by the nanoparticles, which facilitate the transportation of charges [39].

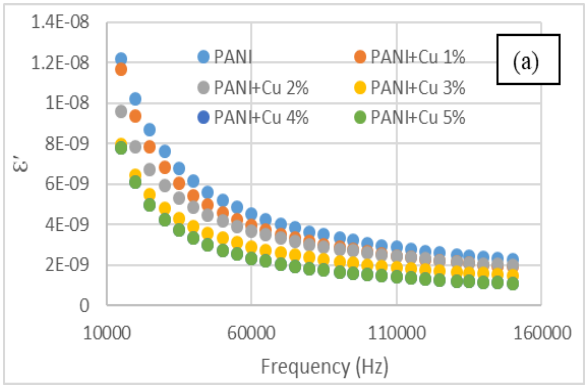

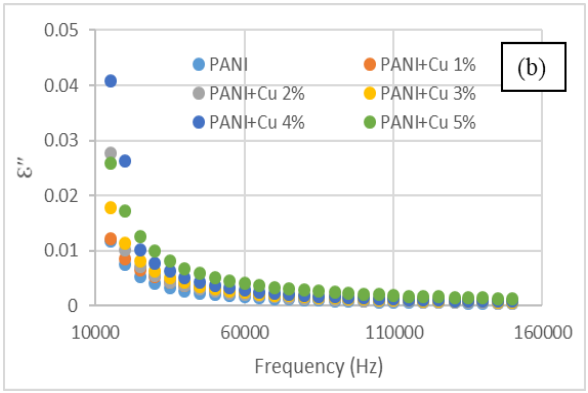

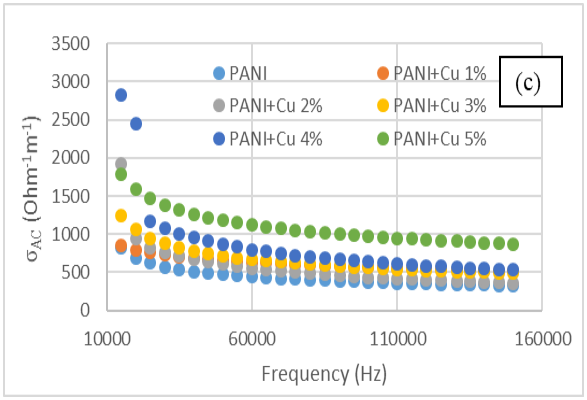

Fig. 6. The values of; (a): real dielectric permittivity ε′, (b): imaginary dielectric ε″ and (c): electrical conductivity σ_{AC} of pure PANI and PANI doped CuNPs samples versus the studied frequency range.

4. Conclusion

The current study confirmed that the PANI doped CuNPs composites were successfully prepared and characterized using various techniques such as Fourier Transform Infrared spectroscopy (FT-IR), X-ray diffraction spectroscopy (XRD), Field Emission Scanning Electron Microscopy (FE-SEM) and Energy Dispersive X-ray spectroscopy (EDS). The absorption peaks in the spectrum of FT-IR showed the interactions between the copper nanoparticles and the molecular chains of polyaniline. The XRD patterns of the PANI doped CuNPs composites detected their crystalline characteristic. The FE-SEM analysis confirmed the uniform distribution of CuNPs in the polymer matrix. In the dielectric study, it was found that the dielectric permittivity values of the PANI doped CuNPs composites are increased compared to the pure PANI and they are decreases with increasing frequency until reach a fixed value at higher frequencies as a result to the interfacial polarization. Furthermore, the electrical conductivity of the PANI doped CuNPs composites also depends

on the frequency. It was high at low frequencies and slowly decreased with rising the frequency until it was nearly constant at high frequencies that attributed to the charge carriers, which are transported during the jumping operations.

5. Acknowledgements

The current work has been supported by Deanship of College of Education for Pure Science- Ibn Al-Haitham and Presidency of Department of Chemistry at University of Baghdad.

6. References

[1] Le T.H., Kim Y., Yoon H., Le T.H., Kim Y., Yoon H., Electrical and electrochemical properties of conducting polymers. *Polymers*, **9**, 150 (2017).

[2] Simotwo S.K., Kalra V., Polyaniline-based electrodes: recent application in supercapacitors and next generation rechargeable batteries, *Curr. Opin. Chem. Eng.*, **13**, 150-160 (2016).

[3] Srivastava S., Kumar S., Kumar Jain V., Vijay Y.K., Effect of temperature on the electrical and gas sensing properties of polyaniline and multiwall carbon nanotube doped polyaniline composite thin films. *Adv Mat Res*. **254**, 167-170 (2011).

[4] Kamel A.H., Amr A.E.G.E., Abdalla N.S., El-Naggar M., Al-Omar M. A., Alkahtani H.M, Sayed A.Y., Novel solid-state potentiometric sensors using polyaniline (PANI) as a solid-contact transducer for flucarbazone herbicide assessment. *Polymers*, **11**, 1796 (2019).

[5] Lee S.Y., Choi G. R., Lim H., Lee K. M., Lee S. K., Electronic transport characteristics of electrolyte-gated conducting polyaniline nanowire field-effect transistors. *Appl. Phys. Lett.*, **95**, 013113(2009).

[6] Tonkin J., Furman J.A., Conducting polymer with enhanced electronic stability applied in cardiac models. *Sci. Adv.*, **2**, e1601007 (2016).

[7] Abdulla H.S., Abbo A.I., Optical and electrical properties of thin films of polyaniline and polypyrrole. *Int. J. Electrochem. Sci.*, **7**, 10666-10678 (2012).

[8] Zhan C., Yu G., Lu Y., Wang L., Wujcik E., Wei S., Conductive polymer nanocomposites: a critical review of modern advanced devices. *J. Mater. Chem. C*, **5,** 1569- 1585 (2017).

[9] Khalil R., Homaeigohar S., Haubler D., Elbahri M., A shape tailored gold-conductive polymer nanocomposite as a transparent electrode with extraordinary insensitivity to volatile organic compounds (VOCs). *Sci. Rep.*, **6**, 33895 (2016).

[10] El-Sheikh M. A., Al-Enezy A., El-Enezy F., Ashammri D., Alrowili W., A novel method for the preparation of conductive methyl cellulose-silver nanoparticles-polyaniline-nanocomposite. *Egypt. J. Chem*, **63**, 8-9 (2020).

[11] Alam M., Ansari A.A., Shaik M.R., Alandis N.M., Optical and electrical conducting properties of Polyaniline/Tin oxide nanocomposite. *Arab. J. Chem.*, **6**, 341-345 (2013).

[12] Jundale D.M., Navale S.T., Khuspe G.D., Dalavi D.S., Patil P.S., Patil V.B., Polyaniline–CuO hybrid nanocomposites: synthesis, structural, morphological, optical and electrical transport studies. *Mater. Sci.: Mater. J.*, **24**, 3526-3535 (2013).

[13] Zahran M., Saleeb M., Elhalawany N., Electrical and dielectrical properties of some novel polyaniline nanocomposites. *Egypt. J. Chem.*, **62**, 1987-1994 (2019).

[14] Tyurnina A.E., Shur V.Y., Kozin R.V., Kuznetsov D.K., Pryakhina V. I., Burban G.V., Synthesis and investigation of stable copper nanoparticle colloids. *Phys. Solid State*, **56**, 1431-1437 (2014).

[15] Zhu H., Zhang C., Yin Y., Novel synthesis of copper nanoparticles: influence of the synthesis conditions on the particle size. *Nanotechnology*, **16**, 3079-3083 (2005).

[16] Khan A., Rashid A., Younas R., Chong R. A chemical reduction approach to the synthesis of copper nanoparticles. *Int. Nano Lett.*, **6**, 21-26 (2016) 21.

[17] Raja M., Subha J., Ali F.B., Ryu S.H., Synthesis of copper nanoparticles by electroreduction process. *Mater. Manuf. Process.*, **23**, 782-785 (2008) 782.

[18] Blosi M., Albonetti S., Dondi M., Martelli C., Baldi G., Microwave-assisted polyol synthesis of Cu nanoparticles. *J. Nanoparticle Res.*, **13**, 127-138 (2011).

[19] Suriati G., Mariatti M., Azizan A., Synthesis of silver nanoparticles by chemical reduction method: effect of reducing agent and surfactant concentration. *Int. J. Automot. Eng.*, **10**, 1920-1927 (2014).

[20] Samim M., Kaushik N.K., Maitra A., Effect of size of copper nanoparticles on its catalytic behaviour in Ullman reaction. *Bull. Mater. Sci.*, **30**, 535-540 (2007).

[21] Shikha J.A.I.N., Ankita J.A.I.N., Kachhawah

P., Devra V., Synthesis and size control of copper nanoparticles and their catalytic application. *Trans. Nonferrous Met. Soc.*, **25**, 3995-4000 (2015).

[22] Huang C.H., Wang H.P., Liao C.Y., Nanosize copper encapsulated carbon thin films on a dye-sensitized solar cell cathode. *J. Nanosci. Nanotechnol.*, **10**, 4782-4785 (2010).

[23] Aguilar M.S., Esparza R., Rosas G., Synthesis of Cu nanoparticles by chemical reduction method. *Trans. Nonferrous Met. Soc.*, **29**, 1510-1515 (2019).

[24] Guo Y., Cao F., Lei X., Mang L., Cheng S., Song J., Fluorescent copper nanoparticles: recent advances in synthesis and applications for sensing metal ions. *Nanoscale*, **8**, 4852-4863 (2016).

[25] Alzahrani E., Ahmed R.A., Synthesis of copper nanoparticles with various sizes and shapes: Application as a superior non-enzymatic sensor and antibacterial agent. *Int. J. Electrochem. Sci.*, **11**, 4712-4723 (2016).

[26] AL-Awadi S.S., Shbeeb R.T., Chiad B.T., Effect of Silver Nanoparticles on Fluorescence Spectra of C480 dye. *Iraqi J. Sci.*, **59**, 502-509 (2018).

[27] Saeed M.A., Ghafoor D.A., Hamid M.K., Yas R.M., Synthesis and Characterization of Gold Nanoparticles by Aluminum as a Reducing Agent. *Baghdad Sci. J.*, **17**, 336-341 (2020).

[28] Samadi N., Hosseini S.V., Fazeli A., Fazeli M.R., Synthesis and antimicrobial effects of silver nanoparticles produced by chemical reduction method. *DARU J. Pharm. Sci.*, **18**, 168–172 (2010).

[29] Padhyay P.K., Ahmad A., Chemical synthesis, spectral characterization and stability of some electrically conducting polymers. *Chinese J. Polym. Sci*, **28**, 191-197 (2010).

[30] Khalid H., Shamaila S., Zafar N., Shahzadi S., Synthesis of copper nanoparticles by chemical reduction method. *Sci. Int*, **2**, 3085-3088 (2015).

[31] Elashmawi I.S., Abdelghany A.M., Hakeem N.A., Quantum confinement effect of CdS nanoparticles dispersed within PVP/PVA nanocomposites. *J Mater Sci: Mater. Electron*, **24**, 2956-2961 (2013).

[32] Naser J.A., Mesomorphic and dielectric properties of heterocyclic liquid crystals with different terminal groups. *Ibn Al Haitham J. for Pure and Appl. Sci*., **29**, 239-253 (2017).

[33] Mututu V., Sunitha A.K., Thomas R., Pandey M., Manoj B., An Investigation on Structural, Electrical and Optical properties of GO/ZnO Nanocomposite. *Int. J. Electrochem. Sci*, **14**, 3752-3763 (2019) 3752.

[34] Naser J.A., Electrical properties of liquid crystalline compounds doped with ferric oxide nanoparticles Fe3O4. *Int J Appl Chem*., 12, 499-511 (2016).

[35] El-Ghamaz N.A., Diab M.A., Zoromba M.S., El-Sonbati A.Z., El-Shahat O., Conducting polymers. VI. Effect of doping with iodine on the dielectrical and electrical conduction properties of polyacrylonitrile. *Solid State Sci.*, **24**, 140-146 (2013).

[36] Marija B.R., Milica V.M., Dejan S.M., Edin H.S., Gordana N.C.M., Maja M.R., Zoran V.S., Influence of TiO2 nanoparticles on formation mechanism of PANI/TiO2 nanocomposite coating on PET fabric and its structural and electrical properties. *Surf. Coat. Technol*., **278**, 38-47 (2015).

[37] Ladhar A., Arous M., Kaddami H., Raihane M., Kallel A., Graça M.P.F., Costa L.C., AC and DC electrical conductivity in natural rubber/nanofibrillated cellulose nanocomposites. *J. Mol. Liq.*, **209**, 272-279 (2015).

[38] El-Sayed S., Mahmoud K.H., Fatah A.A., Hassen A., DSC, TGA and dielectric properties of carboxymethyl cellulose/ polyvinyl alcohol blends. *Physica B Condens. Matter*, **406**, 4068-4076 (2011).

[39] Haneef H.F., Zeidell A.M., Jurchescu O.D., Charge carrier traps in organic semiconductors: a review on the underlying physics and impact on electronic devices. *J. Mater. Chem*, **8**, 759-787 (2020).